Southeast Australia Autumn Rainfall Reduction: A Climate-Change-Induced Poleward Shift of Ocean–Atmosphere Circulation

WENJU CAI AND TIM COWAN

CSIRO Marine and Atmospheric Research, Aspendale, Victoria, Australia

ABSTRACT

Since the 1950s annual rainfall over southeastern Australia (SEA) has decreased considerably with a maximum decline in the austral autumn season (March–May), particularly from 1980 onward. The understanding of SEA autumn rainfall variability, the causes, and associated mechanisms for the autumn reduction remain elusive. As such, a new plausible mechanism for SEA autumn rainfall variability is described, and the dynamics for the reduction are hypothesized. First, there is no recent coherence between SEA autumn rainfall and the southern annular mode, discounting it as a possible driver of the autumn rainfall reduction. Second, weak trends in the subtropical ridge intensity cannot explain the recent autumn rainfall reduction across SEA, even though a significant relationship exists between the ridge and rainfall in April and May. With a collapse in the relationship between the autumn subtropical ridge intensity and position in recent decades, a strengthening in the influence of the postmonsoonal winds from north of Australia has emerged, as evident by a strong post-1980 coherence with SEA mean sea level pressure and rainfall. From mid to late autumn, there has been a replacement of a relative wet climate in SEA with a drier climate from northern latitudes, representing a climate shift that has contributed to the rainfall reduction. The maximum baroclinicity, as indicated by Eady growth rates, has shifted poleward. An associated poleward shift of the dominant process controlling SEA autumn rainfall has further enhanced the reduction, particularly across southern SEA. This observed change over the past few decades is consistent with a poleward shift of the ocean and atmosphere circulation.

1. Introduction

Southeastern Australia (SEA) rainfall in the austral autumn season, March–May (MAM), is known to play an important role in generating annual inflow across the river systems of the region. This is because autumn rainfall acts to wet the catchments after the dry summer season, December–February (DJF), such that followup rainfall in the southern cool seasons of winter, June–August (JJA), and spring, September–November (SON), can be efficiently converted to runoff and catchment inflows (Cai and Cowan 2008a; Murphy and Timbal 2008). Much of the annual inflow into Australia's longest river system, the Murray–Darling basin, is derived from rainfall over SEA. As a result of this autumn wetting mechanism, annual inflow into catchments within the basin are highly sensitive to autumn rainfall variations,

more so than to winter or spring rainfall. As the autumn rainfall reduction (Fig. 1a) in recent decades is largest in terms of either the percentage change of the long-term mean or the absolute total, it has had a severe impact on water availability, made worse by the concurrent rising temperature (Cai and Cowan 2008a; Yu et al. 2010). Much of the rainfall reduction is recorded in April and May (Fig. 1b). In late autumn (i.e., May), rainfall in southern SEA exhibits strong teleconnections with sea surface temperature (SST) variations in the subtropical Indian Ocean and the Timor Sea, north of Australia (Cai and Cowan 2008b); the latter shows a strong coupling with surface pressure in the tropics during May that projects onto the Southern Oscillation index.

The processes influencing southern Australian winter and spring rainfall have been studied extensively. Nicholls (1989) described the separate influence of tropical Pacific and Indian Ocean SSTs on Australian wintertime rainfall. On longer, decadal time scales southern Australian rainfall, particularly over southwest

Corresponding author address: Wenju Cai, CSIRO Marine and Atmospheric Research, PMB 1, Aspendale VIC 3195, Australia.
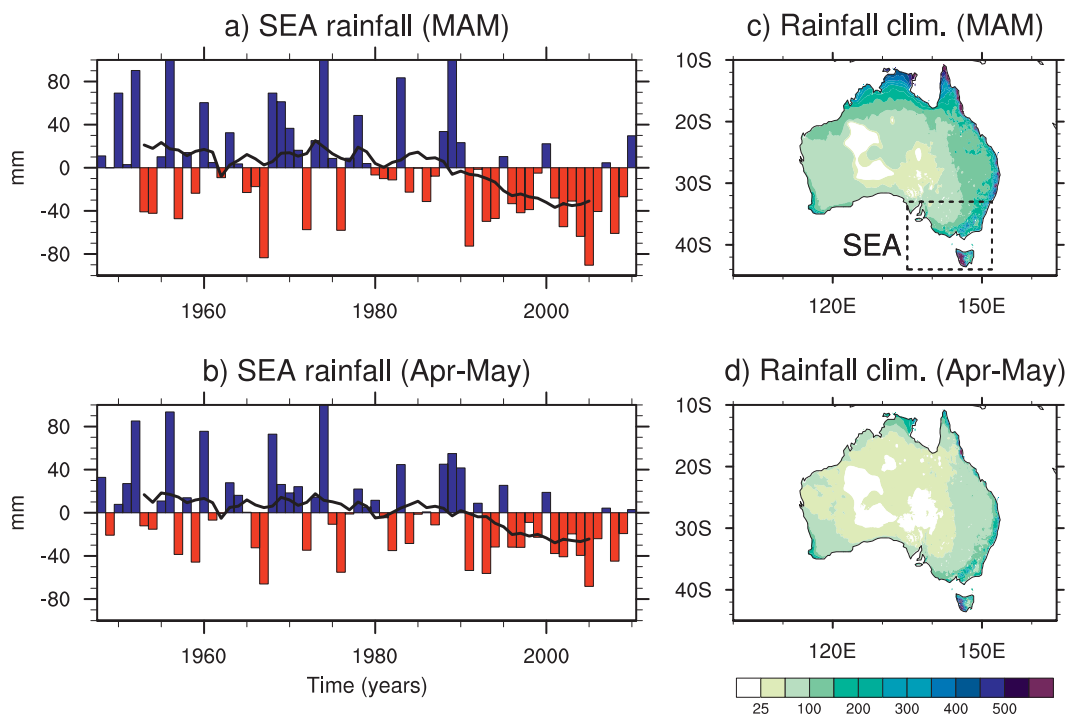E-mail: wenju.cai@csiro.au

FIG. 1. Time series of rainfall anomalies over SEA from 1948 to 2010 for (a) MAM and (b) April–May, fitted with an 11-yr running average (black line). Average Australian rainfall climatology (mm) over 1948–2010 for (c) MAM and (d) April–May. The SEA region is shown in (c), with observations only including land points.

Western Australia (SWWA), is more strongly associated with the local atmospheric circulation than remote Indo-Pacific SSTs (Ansell et al. 2000). However, Indo-Pacific SSTs play an important role in impacting southern SEA through Rossby wave propagation (Cai et al. 2011b). On shorter time scales positive Indian Ocean dipole (IOD) events and the positive phase of the southern annular mode (SAM) both tend to lead to a winter rainfall reduction over southern Australia (Ashok et al. 2003; Cai et al. 2005a; Hendon et al. 2007; Risbey et al. 2009b; Cai et al. 2011b). This is despite the fact that a positive SAM can lead to the development of cutoff low pressure systems, favorable for rainfall across SEA in the cool season (April–October) (Risbey et al. 2009a). In spring the SAM has little impact over southern SEA, except along the central coast of New South Wales where a positive SAM is associated with a rainfall increase (Risbey et al. 2009b), although the IOD and El Niño–Southern Oscillation (ENSO) are important drivers (Cai et al. 2011a). In fact, ENSO conducts its impact through the tropical Indian Ocean via equivalent-barotropic Rossby wave trains, a response that is triggered by anomalous divergence associated with IOD-induced convection anomalies (Cai et al. 2011b). The remote impacts on SEA rainfall of the SAM and the IOD in winter and those of the IOD and ENSO in

spring are projected through local changes in the subtropical ridge intensity (STRI) (Cai et al. 2011a). On the synoptic scale, weather systems that influence rainfall across SEA have been extensively analyzed and are dominated by frontal systems and low pressure cutoff cells (e.g., Risbey et al. 2009a).

In autumn the dynamics controlling SEA rainfall variability and change are less clear, particularly in terms of a tropical influence north of Australia. Using a long-term relationship between the STRI and SEA rainfall, Timbal et al. (2007) argued that the recent increasing STRI could explain about 70% of the observed autumn to mid winter (March–July) SEA rainfall decline. Focusing on autumn only, Cai et al. (2011a) showed that the STRI accounts for only about 11% of the autumn rainfall reduction since 1979. Examining the March–August period over 1958–2007, Nicholls (2009) argued that with respect to southern Australian rainfall the observed trend in the SAM can reproduce over 70% of the observed rainfall trend; without the separation of MAM, it is hard to quantify how much of the cool season rainfall trend is contributed to by the strong coherence between the SAM and southern Australian rainfall in JJA, as is observed over SWWA and SEA (Cai and Cowan 2006; Li et al. 2005; Hendon et al. 2007). Using a separately defined subtropical ridge (STR) over the

entire southern Australia, Larsen and Nicholls (2009) showed that southern Australia autumn rainfall trend is more influenced by a trend in the intensity than the position of the ridge; however, it is not clear to what extent the explained rainfall change is due to the rainfall trend in SEA or in SWWA. Another factor contributing to the rainfall reduction in late autumn is a weakening in the upstream wave train activities (i.e., from the west) that affect downstream rainfall across SEA (Cai and Cowan 2008b).

We therefore confine our analysis to SEA only and initially focus on the average of the autumn months alone (MAM). As outlined above, the main reason why we focus only on SEA is so not to contaminate the analysis with other regions (such as SWWA or eastern Australia) that may have different dominant atmospheric processes controlling rainfall variability. Also, the autumn rainfall decline in SEA is the largest in any season and far greater than in SWWA, and the dynamics of the reduction are not well understood. We separate our analyses into two time periods: 1948–79, denoted as pre-1980, and 1980–2010, denoted as post-1980. The choice of 1980 as a separation year is to encompass the beginning of the long-term reduction in SEA autumn rainfall, particularly in April and May (Fig. 1b), although one could choose the mid-1980s or early 1990s. Choosing 1980 allows for more degrees of freedom to test the level of significance.

We first confirm that the SAM cannot explain the recent SEA MAM rainfall reduction and that the STRI only accounts for a small proportion of the reduction. We then hypothesize that there is an intensification and poleward extension of the dry zone from north of Australia, which in part explains the SEA MAM rainfall reduction (section 3 and 4). In this transition period from monsoon to dry season [i.e., the monsoon typically retreats in March; refer to Kajikawa et al. (2010) and Fig. 6 of the present study], both the intensification and temporal expansion of the dry season could be a contributing factor to a SEA rainfall reduction since 1980. In April and May, regions north of SEA are climatologically drier than SEA latitudes (cf. Figs. 1c and 1d): a shift in the mean climates would result in a reduction in SEA rainfall, particularly across the wetter alpine regions (figure not shown). We then proceed to explore possible processes associated with April and May rainfall variability in the pre-1980 and post-1980 periods (section 5 and 6). We find that there is a poleward shift in the weather systems that influence autumn rainfall variability across SEA. Accompanying this is a southward excursion of the dry autumn climate from latitudes to the north of SEA. We propose that the poleward shift of these systems and the poleward

expansion of the northern dry climate each play a role in the autumn rainfall decline, which is linked to climate change (section 7).

2. Data and methods

To investigate autumn rainfall changes across SEA (south of 33°S, east of 135°E, including Tasmania; see Fig. 1c) we first utilize time series of the STRI and subtropical ridge position (STRP). This data covers the time period 1900–2008, meaning any post-1980 analysis does not cover 2009 and 2010. The STRI is the maximum of the zonally averaged mean sea level pressure (MSLP) over the area of 10°–44°S, 145°–150°E, whereas the STRP describes the latitude where the maximum pressure occurs (Drosdowsky 2005). It should be noted that this definition of the STR may not fully represent the synoptic patterns over the surrounding study region; however, systems that do affect SEA, such as frontal, blocking, and cutoff systems, should have an imprint. We also employ an index of the SAM as defined by Marshall (2003); it is based on MSLP observations so as to avoid the bias in the high latitudes of the Southern Hemisphere seen in assimilated reanalysis products. A measure of the postmonsoonal tropical influence, defined as the northern Australian tropical circulation index (TCI), is constructed by averaging east–west tropospheric winds at 850 mb over a broad area north of eastern Australia (0°–10°S, 120°–150°E). This definition encompasses the region used by Wang et al. (2004) to capture the tropical circulation associated with the Australian summer monsoon, particularly northeastern Australia (NEA). A summer monsoon index described in Kajikawa et al. (2010), averaged over a region northwest of Australia (15°–5°S, 110°–130°E), is shown to capture a higher percentage of the variance of northern Australia summer rainfall but does not fully reflect the well-known reduction in the recent decades. This monsoonal reduction is captured by the Wang et al. (2004) TCI; as such, we use this index to represent the tropical circulation over the region to the north of Australia.

Ocean temperature variations associated with circulation changes are monitored using a global sea ice and SST reanalysis product from the Hadley Centre (Rayner et al. 2003), as well to construct indices of ENSO. Reanalyses from the National Centers for Environmental Prediction (NCEP) (Kalnay et al. 1996) are used to examine the atmospheric circulation anomalies, such as MSLP, atmospheric vertical velocity, and geopotential height fields. Observed monthly gridded Australian rainfall data at a 0.05° resolution, subjected to extensive quality control from the Australian Bureau of Meteorology Research Centre (Jones et al.
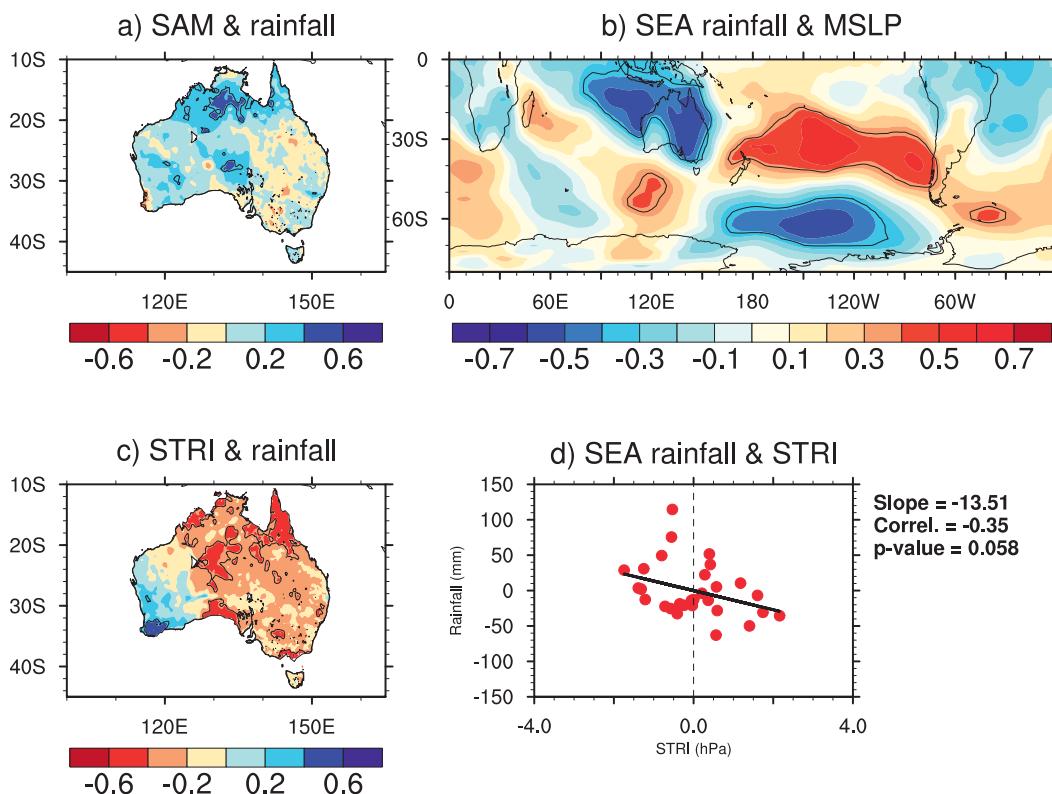
FIG. 2. MAM correlation maps of Australian rainfall with (a) SAM and (c) STRI. (b) Correlation of SEA rainfall and gridpoint MSLP. (d) SEA rainfall vs STRI. All plots cover the period 1979–2008, with significant correlations for (a)–(c) at the 95% confidence level shown within the black contours. The slope, correlation coefficient, and *p* value are given for (d). Please note the color bars in (b) are reversed compared with (a) and (c).

2009), are used to examine the SEA autumn rainfall trend and teleconnections with climate indices. All time series are first linearly detrended to eliminate any coherence generated by long-term trends (e.g., rainfall changes since 1980).

To understand modes of atmospheric variability that impact on SEA autumn rainfall, we conduct empirical orthogonal function (EOF) analysis using a correlation matrix on detrended 500-mb geopotential height (Z_{500}) anomalies in the latitude band 25°–70°S. This latitude band, south of Australia, is a transition zone from the low variance in the tropics to high variance in the high latitudes, reflecting tropical processes and extratropical weather systems. A correlation matrix in effect scales variance everywhere to unity so that the identified mode is not skewed toward the high-latitude process. The extended regional patterns of EOFs are subsequently obtained by a regression analysis using the associated EOF time series. For display purposes, we scale the regression patterns by the one standard deviation anomaly of the EOF time series.

3. The role of SAM and the STR on MAM SEA rainfall variability and trend

a. A lack of a SAM influence

Figure 2a plots the correlation between the MAM SAM index and Australian-wide rainfall; the result shows no significant correlation over the SEA region, consistent with results shown in Meneghini et al. (2007) and Risbey et al. (2009b) for a hemispheric and regionally defined SAM index for this season. The MSLP pattern associated with MAM rainfall variability across SEA does not exhibit a SAM-like structure (Fig. 2b). What it does show in the central Pacific is a pressure pattern that resembles the well-known Pacific–South American (PSA) pattern, while the low pressure center over much of Australia is associated with the Southern Oscillation transitioning into a La Niña–like phase (Cai and Cowan 2008b). It is well known that in winter the SAM has a considerable correlation with rainfall over southern Australia including SEA (e.g., Hendon et al. 2007; Risbey et al. 2009b; Cai et al. 2011a) and SWWA (e.g., Cai and Cowan 2006; Meneghini et al. 2007). By

combining autumn and winter, southern Australia rainfall correlates quite well with the SAM as in Nicholls (2009); however, this result appears to reflect predominantly the winter relationship. As a statistically significant trend exists in the combined autumn–winter SAM, this could account for some of the rainfall trend across southern Australia in the winter months. However, this approach potentially uses the winter SAM–rainfall relationship to explain the MAM rainfall decline, which is not SAM related (Fig. 2a).

b. The role of the STR

One such a possible explanation for the SEA MAM rainfall reduction is the recent upward trend in the STRI since the 1970s (Timbal et al. 2007; Cai et al. 2011a; Larsen and Nicholls 2009). In fact, since around 1980, over the period when much of the MAM rainfall reduction occurs, the coherence between the STRI and SEA rainfall is quite low except over the southern extremities of Victoria (Fig. 2c). In this season a rapid latitudinal shift of the ridge occurs (Larsen and Nicholls 2009) and a change in the timing of seasonal movement of the ridge with a consistent change in synoptic patterns might be important (Frederiksen et al. 2011). Using the SEA MAM rainfall sensitivity to the STRI for the post-1979 period (-13.5 mm hPa^{-1}, Fig. 2d), the intensity only accounts for a small fraction of the total rainfall decline for MAM (about 11%). Will a monthly stratification of the relationship make a difference? Timbal and Hendon (2011) showed that, for the western SEA, April and May rainfall are coherent with the STRI, while Larsen and Nicholls (2009) showed that for the warmer months of November–March the STRI has little impact on southern Australian rainfall.

We analyze the relationship between SEA rainfall and the STRI for March, April, and May separately over the period 1979–2008 (Fig. 3a). The coherence in March is weak and insignificant, consistent with the Larsen and Nicholls (2009) result. For April and May the intensity–rainfall coherence is significant at the 95% confidence level, with sensitivities of -4.08 and -6.02 mm hPa^{-1}, respectively. The spatial patterns associated with the April and May STRI–rainfall relationship shows that there is a broader pattern across SEA for May (Fig. 3c) than for April (Fig. 3b); this relationship has remained stable over the twentieth century (figure not shown) even though the relationship has weakened since the 1960s, particularly in May.

To calculate STRI-induced change in SEA rainfall for the individual autumn months, the STRI–SEA rainfall sensitivities are multiplied by the total STRI trends. Table 1 shows the results with comparisons to the actual SEA rainfall trends. The STRI lacks significant trends in March through May, with April exhibiting the strongest STRI trend in the 30-yr period of 1.79 hPa. Using the sensitivities from Fig. 3a the STRI only accounts for 5.70 mm out of the total 65.85-mm SEA rainfall reduction (or 8.7%), aggregated over the autumn months. This is similar to, but less than, that calculated in Cai et al. (2011a) at 11% for season average, which implies that the STRI cannot explain the recent MAM rainfall changes across SEA. To be able to explain the trend, the sensitivity of rainfall to STRI has to be an order of magnitude greater.

The lack of SEA–STRI rainfall coherence in March compared to April–May further suggests that different forcing factors are responsible for the recent rainfall trends in March as opposed to April–May. As such, we focus on April–May with the intention of explaining the role of the STRI as well as recent changes in the tropical circulation, north of Australia. Below, we describe features associated with the April–May SEA rainfall decline by comparing mechanisms associated with the atmospheric and surface circulation features that control late autumn SEA rainfall variability in the pre and post rainfall-deficit period.

4. Temporal evolution of the relationship between SEA rainfall and circulation indices

a. A weakening STRI–STRP relationship in recent decades

Prior to the late 1960s, there is a statistically significant relationship between the STRI and STRP in April–May, as seen in Fig. 4a, which shows a time series of 30-yr sliding window correlations from 1900 onward. From a historical perspective, a strong STRI–STRP relationship is associated with a strong influence of the STRI on SEA rainfall; this occurs through an impact on the midlatitude storm tracks (Murphy and Timbal 2008). Since around the mid-1960s, the STRI–STRP relationship has weakened considerably, dropping below the 95% significance level in the late 1970s. This collapse is also seen using a separately defined STRI index as described in Larsen and Nicholls (2009) (figure not shown). In late autumn, as the mean midlatitude westerly jets start to migrate northward, the subtropical ridge is establishing itself and the position and intensity become more coherent (Fig. 1 of Cai et al. 2011a). The post-1980 collapse of the STRI–STRP relationship is an important clue for understanding the dynamics of the SEA autumn rainfall reduction. A process that can influence the establishment of the STR is an extension of the northern dry season, following the retreat of the Australian summer monsoon.
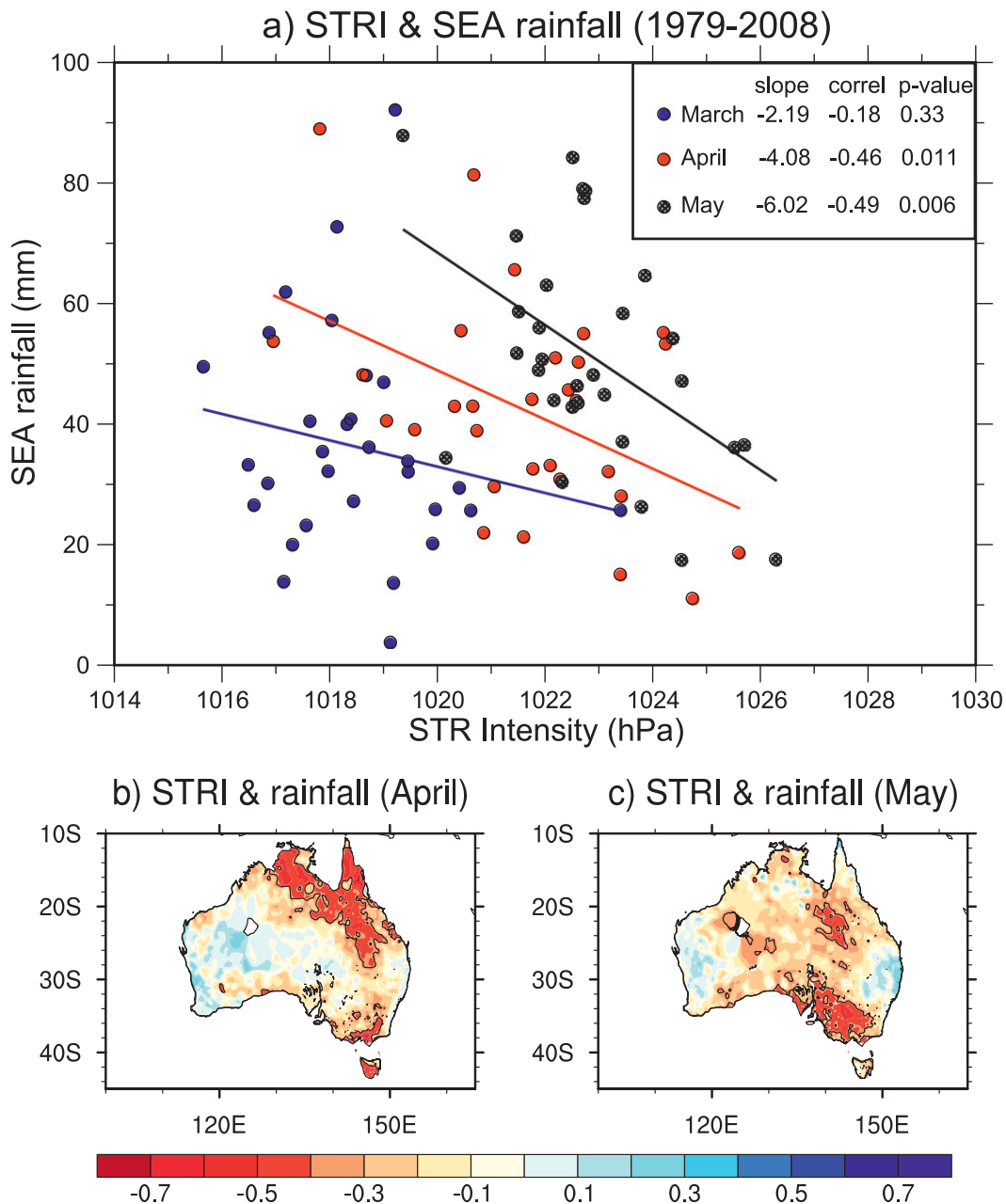
FIG. 3. (a) Scatterplot between STRI and SEA rainfall (both detrended) for separate autumn months over 1979–2008; correlation maps of Australian rainfall with STRI (both detrended) in (b) April and (c) May, over 1979–2008. Slopes, correlation coefficients, and *p* values for (a) are listed with values of p less than 0.05, indicating statistical significance of slopes at the 95% confidence level. Significant correlations for (b) and (c) at the 95% confidence level are shown within the black contours.

b. A strengthening influence from the northern climate

The Australian monsoon reversal and retreat to the dry season typically occurs during early autumn, typically in March (Smith et al. 2008; Zhang 2009). Prior to the 1980s, the northern tropical influence, as represented by the TCI, on SEA rainfall is weak and not statistically significant (Fig. 4c). The coherence of the TCI with local pressure is also much weaker prior to 1990, although it is statistically significant from 1970 onward (Fig. 4b). As such, SEA rainfall shows a distinct lack of spatial coherence with rainfall across NEA in the pre-1980 period (Fig. 5a),

TABLE 1. Monthly autumn sensitivities of SEA rainfall associated with the STRI, as well as trends of STRI, STRI-induced SEA rainfall, and SEA rainfall over 1979–2008. Significant trends above the 95% confidence level based on a two-tailed t test are shown in italics.

	Sensitivity (mm hPa^{-1})	STRI trend [hPa (30 yr)$^{-1}$]	STRI-induced rain trend [mm (30 yr)$^{-1}$]	SEA rainfall trend [mm (30 yr)$^{-1}$]
Mar	−2.19	0.10	−0.23	−19.09
Apr	*−4.08*	1.79	−7.32	−20.70
May	*−6.02*	−0.31	1.84	*−26.06*
Total	−12.29	0.54	−5.70	*−65.85*

reflecting the fact that it is not strongly influenced by the tropics. Instead it shows a stronger coherence with regional rainfall from southern South Australia, to the west of SEA (e.g., the Eyre Peninsula; ~34°S, 136°E). There is also a lack of a significant tropical circulation-induced MSLP teleconnection across SEA, with correlations reflecting local tropical variations (Fig. 5b).

In the post-1980 period, the imprint of the TCI extends to SEA latitudes, enabling it to influence rainfall through local pressure changes (Figs. 4b,c, shaded sections). As such, SEA April–May rainfall is more coherent with rainfall north of SEA including part of northern Australia (Fig. 5c), and MSLP anomalies associated with the TCI extend poleward to the SEA region (Fig. 5d). This increasing broad-scale rainfall coherence across much of eastern Australia suggests that the circulation anomalies from the north are extending poleward. Much of this tropical signal incursion occurs after 1990 (Fig. 4c), a period where no large anomalously wet April–May months have been observed (as of 2010).
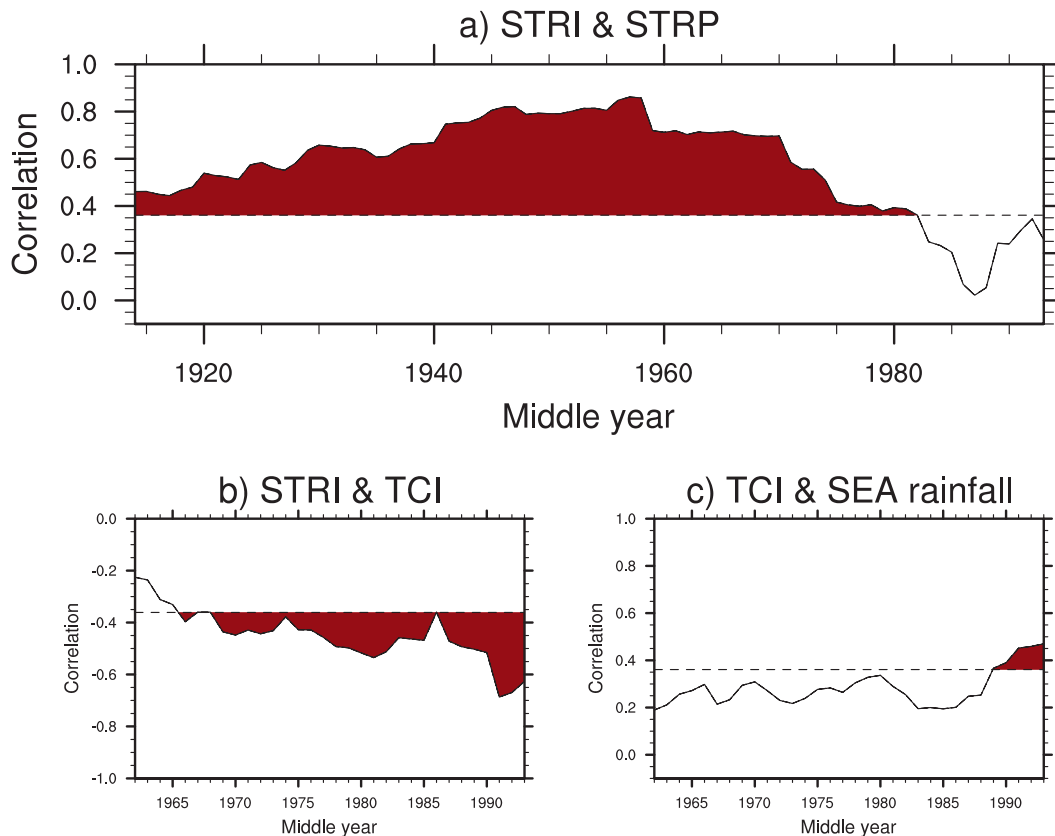

FIG. 4. Thirty-year sliding window of April–May correlations: (a) STRI with STRP, (b) STRI with a northern Australian tropical circulation index (TCI), and (c) TCI with SEA rainfall. The TCI is defined as the average zonal 850-mb winds over an area north of Australia (0°–10°S, 120°–150°E). The shaded regions indicate significance at the 95% confidence level.
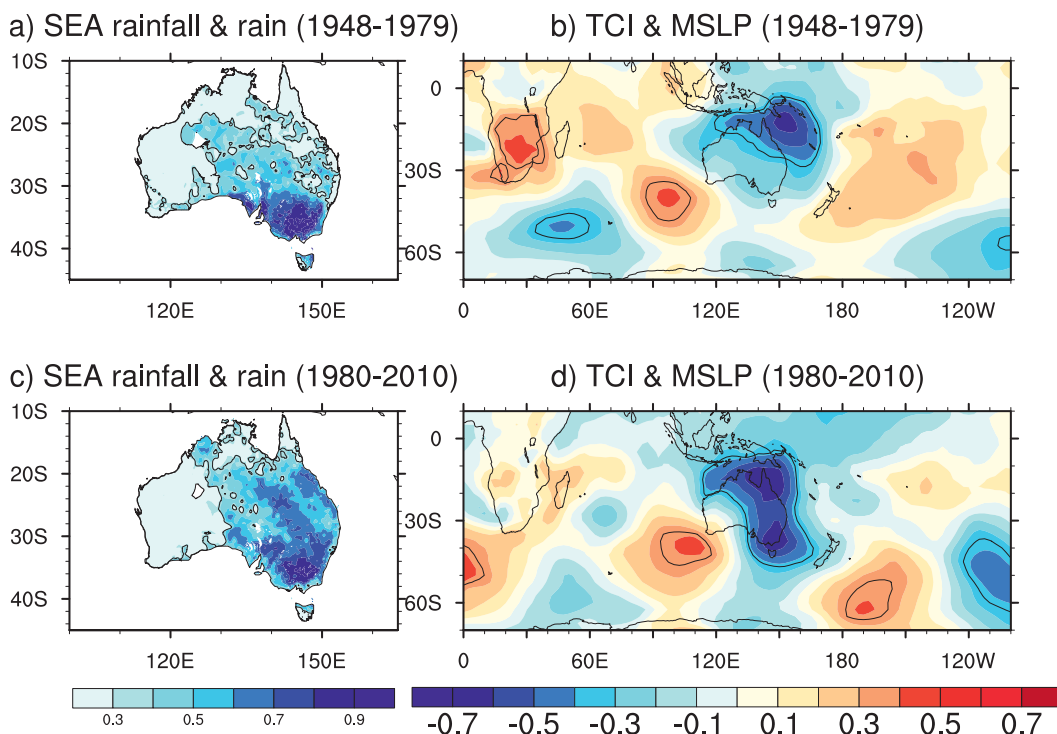
FIG. 5. April–May correlations of (a) SEA rainfall with Australian-wide rainfall and (b) TCI with gridpoint MSLP, for the period 1948–79; (c),(d) as above but for 1980–2010. Significant correlations at the 95% confidence level are within the black contours.

c. A changing northern climate in recent decades

The northern dry transition season (autumn) itself has undergone significant decadal changes since the late 1940s. First, the TCI has weakened since the mid-1970s (Fig. 6, main plot); that is, the dry season is becoming dominated by stronger easterly flow. Second, by early to mid March, the monsoon retreat (or reversal) has typically occurred; however, in recent decades this has been commencing earlier (Fig. 6, small panel). This temporal expansion means that the increasing TCI influence on SEA MAM rainfall is not a rain-inducing process for SEA. This is because, in terms of the long-term climatology, April and May rainfall north of SEA, including tropical northern Australia, is lower than that over SEA (Fig. 1d). Therefore, any poleward expansion of the northern dry climate would contribute to the rainfall decrease through replacing a climatologically wet regime with a dry one experienced in latitudes to the north of SEA.

d. A historical perspective of the recent northern climate influence

We next investigate the historical significance of this recent poleward extension of the northern dry autumn climate. Taken from the NCEP reanalysis, the TCI record begins in 1948 when the reanalysis data commences. As the NEA rainfall (averaged over Australia land points 10°–20°S, 140°–150°E) correlates well with the TCI (Fig. 7a), we take NEA rainfall as a surrogate for the TCI. In doing so, we can extend the proxy TCI back to 1900 when Australian rainfall records began. A time series of correlations between SEA and NEA rainfall using a 30-yr sliding window indicates that the recent decades have shown the strongest coherence in over 100 years of records (Fig. 7b), reflecting the uniqueness of the poleward extension of the northern dry-season influence over the past three decades. Adding to this, during the past 30 years (1980–2010, for April–May) the coherence between central SEA rainfall and rainfall across southern South Australia (i.e., rainfall to the west of SEA) has fallen to below the 95% significance level, not observed since the 1920s (figure not shown). While the dynamics are not clear, it may be associated with a widening of the Hadley cell circulation and its subtropical edges (e.g., Hu and Fu 2007; Johanson and Fu 2009; Cai and Cowan 2012), as well as a poleward shift in the extratropical weather systems (e.g., Frederiksen et al. 2011).
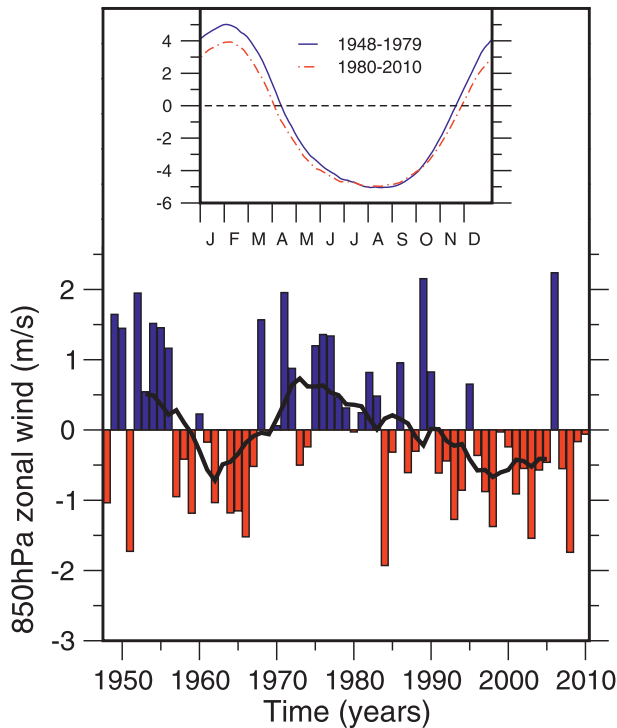
FIG. 6. (bottom) Time series of the TCI, fitted with an 11-yr running mean (black line), with (top) the annual cycles of the TCI for the periods 1948–79 (blue) and 1980–2010 (red).

5. A poleward shift of circulation modes of atmospheric variability

Section 4 presented evidence of an enhanced coherence between the tropical and extratropical circulation to support a poleward extension of the subtropical dry climate in April–May. In this section, we show that the enhanced coherence is accompanied by a poleward shift in the modes of variability affecting SEA April–May rainfall.

a. The pre-1980 period (1948–79)

As discussed by Cai and Cowan (2008b), there is no known mode of SST variability in late autumn that acts as a potential dominant driver for rainfall variability. We therefore turn our attention to the atmospheric modes, applying EOF to Z_{500} anomalies over the pre-1980 period, as described in section 2, and then regressing the raw Z_{500} anomalies onto the Z_{500} EOF time series.

The dominant mode accounts for 21.1% of the total variance and incorporates two equivalent-barotropic Rossby wave trains that propagate from the east and west subtropical Indian Ocean. These curve poleward west of the Drake Passage and then equatorward to the east; the wave train triggered in the east Indian Ocean displays a low pressure center over southern Australia
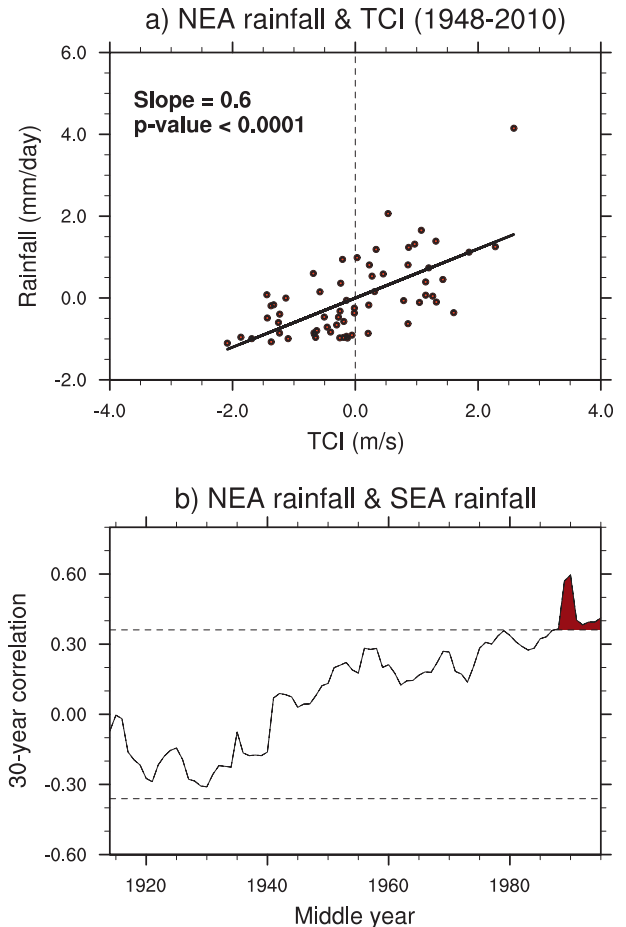

FIG. 7. (a) Scatterplot of April–May rainfall anomalies over NEA (averaged over 10°–20°S, 140°–150°E) against the TCI for the period 1948–2010; a line of best fit is also shown. (b) Thirty-year sliding window correlation of northeast Australian rainfall and SEA rainfall. The shaded region indicates significance at the 95% confidence level.

(Fig. 8a). These two wave trains appear to share a low pressure center farther downstream to the west of the Drake Passage and can be regarded as an aggregate of the synoptic weather systems on a seasonal time scale; indeed, this mode is correlated with April–May rainfall over much of SEA and parts of NEA (Fig. 8d). In contrast, there is no influence along the eastern coastal regions, reflecting the likelihood of different rainfall producing systems associated with the Pacific decadal oscillation influencing this region (e.g., Speer et al. 2011). This mode also contributes to variations in the STRI; the pre-1980 correlation is −0.62, statistically significant at the 99% confidence level.

The second Z_{500} (EOF2), which accounts for 15.4% of the total variance, has a SAM-like pattern (Fig. 8b) with a strong zonal structure in the extratropics. The edge of
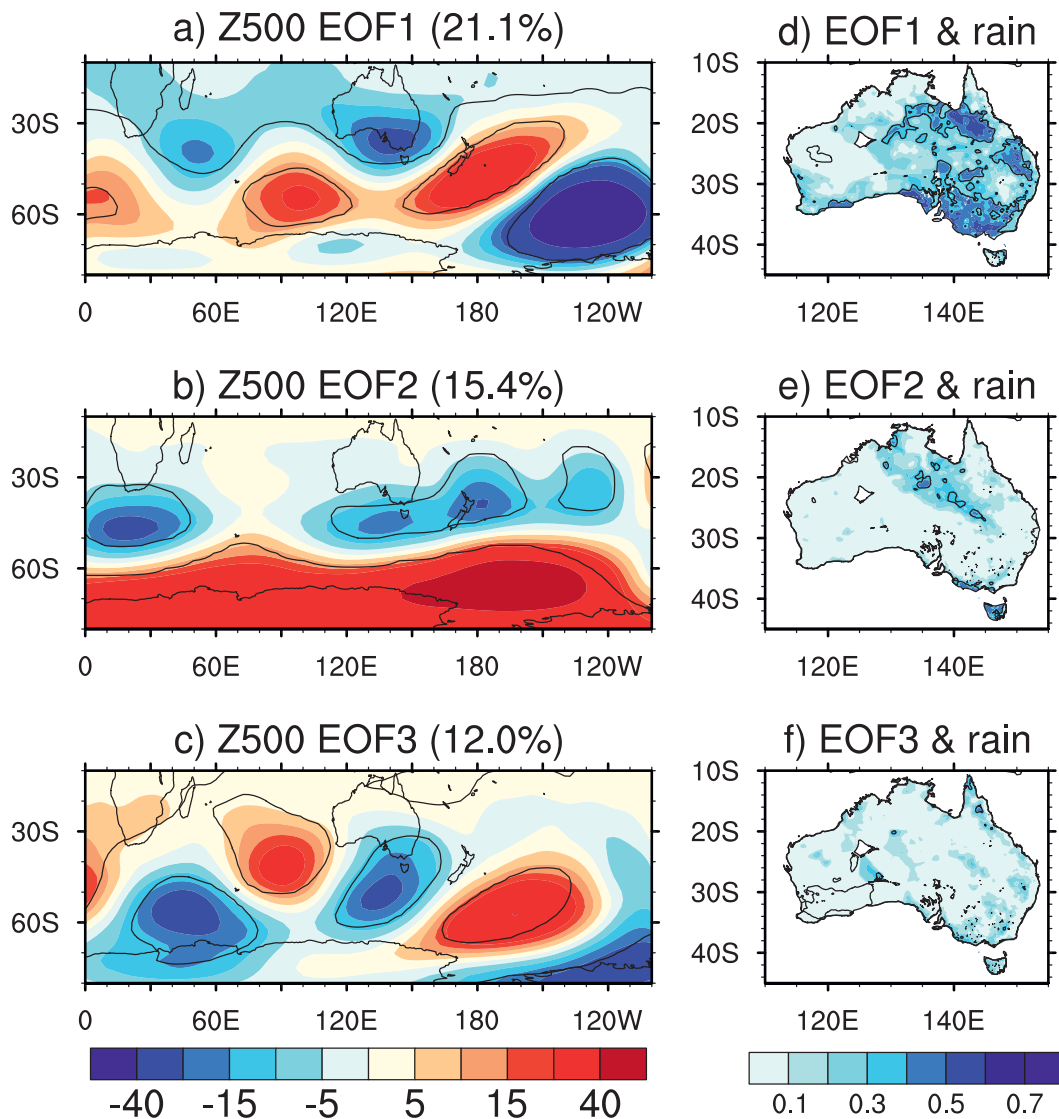
FIG. 8. April–May one standard deviation anomaly patterns of Z_{500} (m) associated with (a) EOF1, (b) EOF2, and (c) EOF3 over 25°–70°S latitude band for 1948–79; (d)–(f) The spatial correlation maps between Australian rainfall and the respective EOF time series (both detrended). The variance explained by each mode is shown in the figure title in (a)–(c). Significant correlations at the 95% confidence level are within the black contours.

low pressure band associated with the second mode extends to Tasmania and the southern fringes of SEA and therefore displays little coherence with SEA April–May rainfall (Fig. 8e). It is also not strongly correlated with the STRI (-0.33). The third Z_{500} mode (EOF3), accounting for 12.0% of the total variance, has a quasi-wavenumber-4 pattern with a low pressure center rimming SEA from the south (Fig. 8c). This mode has little impact on SEA rainfall (Fig. 8f) because a setting of a high pressure center to the west of SWWA supports equatorward winds inhibiting tropical high moisture-laden airflow, unfavorable to rainfall over the region. This

mode is correlated (-0.39) with the STRI just surpassing the 95% confidence level.

These three modes may be regarded as the atmospheric circulation modes that potentially influence the SEA region in April–May: Z_{500} EOF1 and EOF3 represent the "tracks" of synoptic systems—EOF1 is from the northwest, that is, the tropical Indian Ocean (likely in terms of northwest cloud band events), and EOF3 represents westerly weather systems from the southern Indian Ocean but appears to be too far south to influence SEA rainfall, showing no correlation with SEA rainfall. The Z_{500} EOF2 represents a regional SAM-like
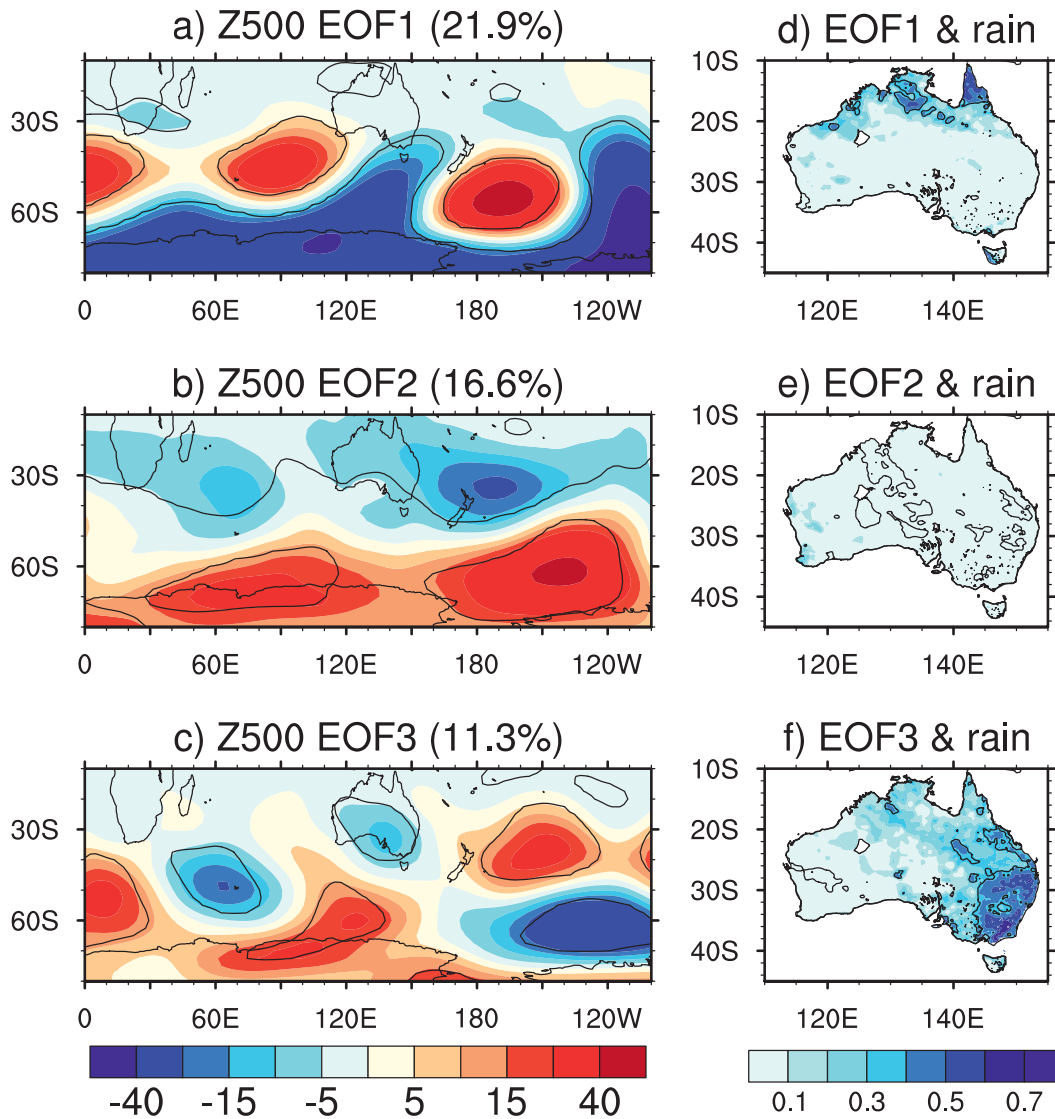
FIG. 9. As in Fig. 8 but for 1980–2010.

pattern, similar to that described in Meneghini et al. (2007), who showed that a regionally defined SAM has little association with SEA MAM rainfall.

b. The post-1980 period (1980–2010)

A similar analysis in the post-1980 period yields three equivalent EOFs, with the dominant mode (EOF1, Fig. 9a), accounting for 21.9% of the total variance, appearing to be the equivalent of the pre-1980 EOF3 (Fig. 8c). The spatial patterns of the post-1980 EOF1 and pre-1980 EOF3 patterns show resemblances, with a weighted pattern correlation of 0.66 (0.70 unweighted), except that there is a clear poleward shift in the height centers. As a result of the shift, the low pressure near the SEA region is far weaker and does not extend as far northward. That

the pattern becomes the dominant mode, which is confirmed by separate composite analysis (figure not shown), is an indication of a systematic poleward shift in the wave train with much of the variance now occurring in the higher (southern) latitudes. Again, there is a corresponding lack of rainfall correlations over SEA, although there is a rainfall signal present along the west coast of Tasmania (Fig. 9d). The importance of the wave train poleward shift accompanying the poleward expansion of the dry zone in explaining the SEA autumn rainfall reduction will be examined in section 6. This post-1980 EOF1 mode has a weak correlation with the STRI (-0.16; this is for 1980–2008, the period for which we have STRI data). The mode incorporates variability in the tropics with significant rainfall correlations

over northern Australia, for which the dynamics are unclear.

The second EOF again showing a SAM-like pattern (Fig. 9b; variance 16.6%), with a low pressure belt shifted northward. As a consequence, the flow is southeasterly, directing cool dry air to eastern Australia and generating negative rainfall anomalies across eastern Australia (Fig. 9e); however, the correlations do not extend to SEA.

The third mode (EOF3) in the post-1980 period, which accounts for 11.3% of the total variance, shows an imprint of the pre-1980 EOF1 equivalent, but with two altered features (Fig. 9c). First, the upstream anomaly center in the Indian Ocean sector has shifted poleward from 40°S in the pre-1980 period (Fig. 8a) to 45°–50°S (Fig. 9c), along with the positive anomaly center downstream (~60°S, 120°E). Second, there is no poleward curling Rossby wave train emanating from the tropical east Indian Ocean; instead, there is a single anomaly center over Australia, which represents the extratropical equivalent-barotropic signal linked to a strengthened poleward expansion of the dry zone discussed in section 4 and shown in Fig. 5d. In the South Pacific the EOF3 mode incorporates a PSA pattern, which in part reflects the atmospheric response to SST anomalies in the tropical Pacific (Karoly 1989; Ghil and Mo 1991). The PSA anomaly centers are situated too far away from Australia and do not have a pathway to impact SEA rainfall, not unlike ENSO in winter and spring (e.g., Cai et al. 2011a,b). The upstream poleward-shifted anomaly centers do not influence Australian rainfall either. Therefore, it is the poleward expansion of the northern Australia dry-season influence imbedded in this mode that leads to considerable post-1980 rainfall correlations over the SEA region (Fig. 9f), as projected in part through the STRI. In fact, correlations of the post-1980 EOF3 with the STRI are −0.46, statistically significant above the 95% confidence level and consistent with Fig. 4b.

To summarize, since around 1980 there is a poleward expansion of the dry-zone, with a direct influence on SEA rainfall in mid to late autumn. Accompanying the change is a poleward shift in modes of variability. Prior to 1980 variations associated with EOF1, which consists of two signals emanating from the tropical Indian Ocean, lead to anomalously wet and dry autumns across SEA. Since 1980 the mode of variability that describes westerly weather systems from the southern Indian Ocean (EOF3 in the pre-1980 period) has become the more dominant mode, effectively replacing the tropical Indian Ocean mode. Both of these modes have exhibited a poleward shift since 1980, and the westerly weather system mode is too far south of SEA to influence rainfall over the region. This, in effect, leaves dry conditions caused by the poleward expansion of the dry zone unmodulated, therefore resulting in a persistent drought as has been observed in autumn since the 1980s.

To support our argument of a poleward shift, we have calculated the Eady growth rate (a measure of baroclinicity in the development of weather systems; see Simmonds and Lim 2009; Risbey et al. 2009a) for April and May separately using NCEP monthly output. The results (Fig. 10) highlight the changes in the 500-hPa (midtroposphere) zonally averaged Eady growth rate between the post-1980 and pre-1980 periods. Reductions (in red) in the growth rate are seen across much of the midlatitude band, predominantly upstream from Western Australia. The zonal-mean total Eady growth rate for each period shows that the maximum baroclinicity (~50°S) is located farther poleward in the latter period compared to the pre-1980 period.

6. SST anomalies associated with the atmospheric modes

To explore the nature of atmospheric–oceanic processes associated with the atmospheric circulation modes in April–May, we correlate gridpoint SST anomalies with SEA rainfall and Z_{500} EOF time series. The correlation analysis is separated into each of the two analysis periods, 1948–79 and 1980–2010.

a. The pre-1980 period

Prior to 1980, SST anomalies associated with SEA rainfall and Z_{500} EOF1 display a similar pattern in subtropical Indian Ocean and Tasman Sea regions (Figs. 11a,b). Both show a subtropical Indian Ocean dipole-like pattern, although the position and scale of the poles are slightly different from those identified by previous studies (e.g., Behera and Yamagata 2001; Reason 2001; Fauchereau et al. 2003; Hermes and Reason 2005); for example, the subtropical Indian Ocean dipole (SIOD) in these studies features a southern pole with a broader spatial scale that peaks in austral summer and extends to Madagascar. The pattern associated with EOF1 (Fig. 11b) initially suggests that a La Niña–like circulation with a basinwide Indian Ocean cooling is conducive to modulating SEA rainfall. However, the pattern associated with SEA rainfall (Fig. 11a) indicates that the influence of ENSO is only weak and that the SIOD is the central feature associated with SEA rainfall variability, a feature already described for the month of May (Cai and Cowan 2008a).

The Z_{500} EOF3 pattern that affects rainfall over southwest SEA and western Tasmania is also associated with a dipolar SST pattern (Fig. 11c), in line with the notion of an atmospheric forcing on the ocean
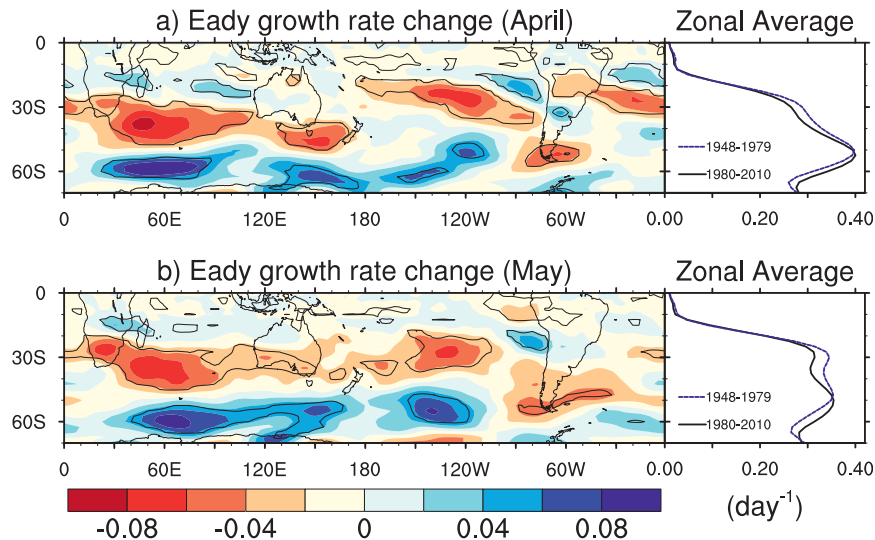
FIG. 10. The 500-hPa Eady growth rate difference between the post-1980 and pre-1980 period (post-1980 minus pre-1980) and the zonal mean of the total Eady growth rate for each period for (a) April and (b) May, based on NCEP. The Eady growth rate (day^{-1}) is calculated on the Simmonds and Lim (2009) definition and measures baroclinic instability favorable for the development for storm systems (Risbey et al. 2009a).

(Fauchereau et al. 2003; Hermes and Reason 2005). The dipole-like pattern is consistent with the positive height anomalies over the Indian Ocean (Fig. 8c), with its cold pole trapped near the midwest Australia coast (Fig. 11c). Thus, a dipole pattern appears common during April and May. It is worth noting that the cold pole does not extend into the tropical Indian Ocean and thus does not "tap" into tropical SSTs that can induce a Rossby wave train as for EOF1.

In the patterns associated with SEA rainfall and Z_{500} EOF1 (Fig. 11b), the cold pole extends into the equatorial Indian Ocean where convective activity is strong. The cooling maximum is situated in the central equatorial Indian Ocean: that is, with equivalent relative warming to the two sides of the cooling center, where the two Rossby wave trains are triggered (Fig. 8a). The generation of Rossby wave trains appears consistent with the notion that upper-tropospheric divergence anomalies resulting from tropical convection variations act as a Rossby wave source. Although the process requires detailed examination, it is plausible that the Rossby wave trains in turn act to maintain the dipole: the high pressure center southwest of Australia and the low pressure anomaly center to the northeast (as in Fig. 8a) drive a southeasterly flow of cool air that is conducive to the cold SST anomaly. To the south the same high pressure anomalies generate warm northerlies west of the high pressure center that in turn act to promote warm SST anomalies.

b. The post-1980 period

In the post-1980 period, the SST anomaly patterns associated with SEA rainfall and Z_{500} EOF3 also share some commonalities, including a warm anomaly to the north of Australia (120°E eastward) and the absence of an involvement of the warm SST anomalies in the extratropical Indian Ocean (Figs. 11d,e). The warm anomaly to the north of Australia is consistent with a dry-season influence direct from northern Australia. As in the pre-1980 period, there is no pathway for ENSO to influence SEA April–May rainfall because the ENSO-related anomaly centers are remotely located in the central Pacific. SEA rainfall in these two months is associated mainly with a tropical SST signal to the north of Australia (Figs. 11d,e). The pattern associated with the post-1980 EOF3 displays a weak ENSO-like structure (Fig. 11e), reflecting that some of the ENSO-induced PSA pattern projects onto this mode (Fig. 9c).

A SIOD-like pattern also exists in the post-1980 period, incorporated in the SST pattern associated with Z_{500} EOF1 (Fig. 11f). This post-1980 EOF1 is fundamentally different from the pre-1980 EOF1 SST pattern (Fig. 11b) in that the associated cold pole does not extend into the tropical Indian Ocean (Fig. 11f); in association, there is a lack of tropical convection anomalies that can induce a Rossby wave train from the Indian Ocean. This being the case, we postulate that the post-1980
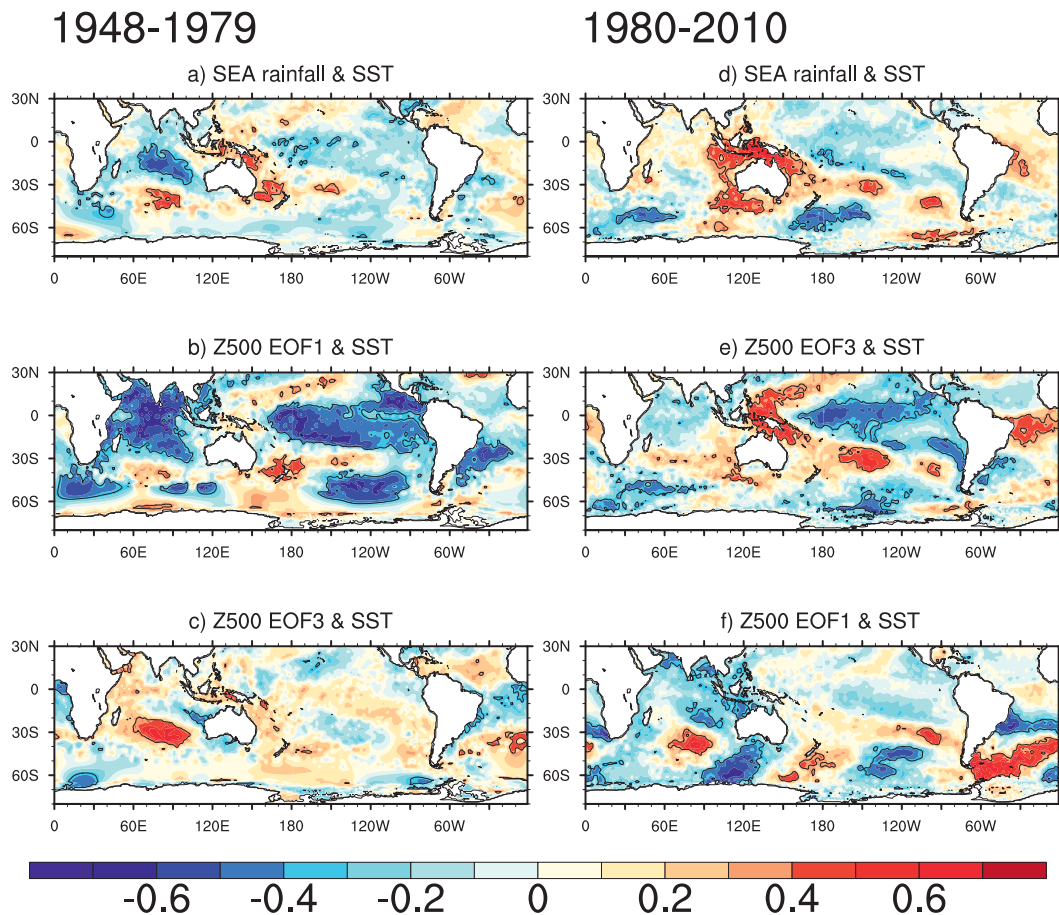
1948-1979   1980-2010

FIG. 11. April–May correlation maps of gridpoint SST with (a) SEA rainfall, (b) Z_{500} EOF1, and (c) Z_{500} EOF3, over the period 1948–79; as above but for 1980–2010 with (d) SEA rainfall, (e) Z_{500} EOF3, and (f) Z_{500} EOF1. Significant correlations at the 95% confidence level are within the black contours.

Z_{500} EOF1 is a poleward shift of the pre-1980 Z_{500} EOF3; this is further discussed in the next section.

7. Discussion

a. The post-1980 circulation poleward shift

The dipole structure identified in the pre-1980 period (Figs. 11a,b) is almost identical to that associated with the austral summer SIOD identified in previous studies (e.g., Fauchereau et al. 2003; Hermes and Reason 2005). These studies argue that the atmosphere forces the ocean during subtropical dipole events through wind-induced changes to the surface latent heat fluxes. They confirm this idea of "an atmosphere forcing on the ocean" through lag correlations between atmospheric circulation fields and SST anomalies, with the former leading the latter. Although this mode is most pronounced in the austral summer, it extends into the autumn season.

Linking the austral summer SIOD to a similar dipolelike pattern in the South Atlantic (e.g., Venegas et al. 1997), Fauchereau et al. (2003) further show that there are concurrent SST anomalies in the midlatitude South Pacific during strong SIOD events. They find that the SST anomalies are induced by a systematic anomalous southward (northward) shift and strengthening (weakening) of the entire subtropical high pressure systems on interannual time scales [e.g., the St. Helena anticyclone in the Atlantic Ocean and Mascarene anticyclone in the Indian Ocean, see Fig. 7 of Fauchereau et al. (2003)]. On such time scales, such a shift would generate a system of global SST anomalies in all three oceans. By analogy, we would expect a well-defined system of concurrent SST anomalies in the three oceans to be associated with the post-1980 EOF1 if it is in fact reflecting the poleward-shifted pattern of the pre-1980 EOF3.

This is indeed the case. The poleward shift is confirmed by comparing SST anomalies associated with

these two modes (Figs. 11c,f). There is a poleward shift of the SIOD, with the warm center located about 5° farther poleward, as well as better-defined SST anomalies in all three southern ocean basins, than seen in the pre-1980 period. These downstream anomalies are present in the pre-1980 period but are weak and situated farther northward. The shifted anomaly system in the post-1980 period strongly resembles that shown in Fig. 5 of Fauchereau et al. (2003), although they focused on austral summer months (November–February). The setting is consistent with northerly (southerly) flows over the warm (cold) SST anomalies.

b. Possible linkage to climate change

We have shown that accompanying the poleward shift of the Rossby wave train systems is the poleward expansion of the dry zone in the early northern dry season, with this expansion the strongest in recent decades (Fig. 5d). It is likely that the poleward shift of the wave train pattern may facilitate the poleward expansion of the dry zone and vice versa, but it is possible that they may be a response to a common forcing. This forcing may also be responsible for a positive trend in the SAM. Indeed, there is evidence supporting that all of these phenomena are at least in part a consequence of global climate change.

A poleward shift is found in the surface wind stress curl, which is dominated by the meridional gradient of the east–west wind stress. In such a curl field, the zero-curl line in the subtropics marks the location where the subtropical oceanic gyre separates from the Antarctic Circumpolar Current, and the zonal average of the curl indicates the strength of the gyre circulation at a given latitude. A Hovmöller diagram of the zonal averages of the curl for April–May clearly show a poleward shift and intensification of the global gyre circulation (Fig. 12), particularly south of 40°S. Plots for each individual ocean display similar features (figure not shown), with the poleward intensification strongest in the early 1980s.

Recent studies have shown that such a poleward shift and intensification of the gyre circulation is congruent with recent wind changes associated with the upward trend of the SAM (e.g., Cai et al. 2005b; Cai 2006; Cai and Cowan 2007). Such a poleward shift in the curl is a robust feature of the late twentieth century climate simulations from models that participated in phase 3 of the Coupled Model Intercomparison Project (CMIP3) (Cai and Cowan 2007). Studies, both observational and model based, also suggest that the upward trend of the SAM is mostly induced by Antarctic stratospheric ozone depletion (Thompson and Solomon 2002; Gillett and Thompson 2003; Miller et al. 2006). Using CMIP3
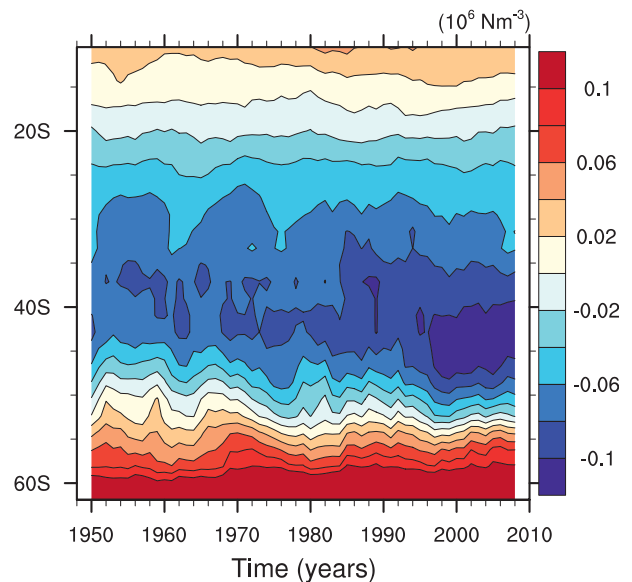

FIG. 12. Zonally averaged wind stress curl for April–May over the period 1948–2010, smoothed using a 5-yr running average.

climate model outputs, Cai and Cowan (2007) further quantified the relative contribution from Antarctic ozone depletion and increasing anthropogenic greenhouse gases and found that about two-thirds of the observed SAM trend over 1950–99 is attributable to ozone depletion, with the remainder induced by increasing greenhouse gases such as CO_2. In association, the sinking branch of the Hadley cell is now located farther poleward (Lu et al. 2007; Fu et al. 2006; Kang et al. 2011).

As previously shown for autumn, the SAM has no influence on southern Australia rainfall (Fig. 2a); however, the wave train modes (pre-1980 EOF1) show strong teleconnections, together reflecting the meridional variations of the atmospheric circulation. As these wave train systems shift poleward, so do the "centers of action" of these modes. Given that the upward trend of the SAM and the poleward shift of the mean circulation are at least in part induced by climate change, it is likely that the poleward shift of the modes is partly attributable to climate change, particularly Antarctic stratospheric ozone depletion.

8. Conclusions

The present study describes mechanisms of SEA autumn rainfall variability in the post-1980 period when a substantial decline occurs. We first confirm that there is no relationship between SEA autumn rainfall and the SAM, while the relationship between the autumn STRI

and SEA rainfall is weak. As such, the autumn rainfall reduction across SEA cannot be explained by changes in the SAM or the STRI. Further, we show that, while there is a disassociation between the STRI and STRP in recent decades, the influence of the northern dry-season circulation is strengthening, as highlighted by a stronger coherence of the TCI with the STRI and SEA rainfall. Climatologically, autumn rainfall over the TCI region north of SEA and northern Australia, particularly during April and May when the monsoon has retreated/reversed, is lower than that in the SEA region. Moreover, the northern dry season has been getting drier and retreating earlier since the 1980s. Thus an intensifying influence in the northern dry season is considered a contributing factor to the SEA autumn rainfall reduction. In association there has been a poleward shift in the dominant atmospheric modes that influence SEA autumn rainfall variability, from the pre-1980 systems emanating from the west and the northwest to the post-1980 regime dominated by the northern dry-season influence. The poleward shift of these variability modes means that a drought-breaking process is not operating as frequently as before. This change is consistent with a poleward shift of the ocean and atmosphere circulation observed over the past decades and is at least in part attributable to climate change. Thus, the possibility that the recent multidecade-long autumn rainfall reduction over SEA bears an imprint of anthropogenic climate change should be considered.

REFERENCES

Ansell, T. J., C. J. C. Reason, I. N. Smith, and K. Keay, 2000: Evidence for decadal variability in southern Australian rainfall and relationships with regional pressure and sea surface temperature. *Int. J. Climatol.,* **20,** 1113–1129.

Ashok, K., Z. Guan, and T. Yamagata, 2003: Influence of the Indian Ocean dipole on the Australian winter rainfall. *Geophys. Res. Lett.,* **30,** 1821, doi:10.1029/2003GL017926.

Behera, S. K., and T. Yamagata, 2001: Subtropical SST dipole events in the southern Indian Ocean. *Geophys. Res. Lett.,* **28,** 327–330.

Cai, W., 2006: Antarctic ozone depletion causes an intensification of the Southern Ocean super-gyre circulation. *Geophys. Res. Lett.,* **33,** L03712, doi:10.1029/2005GL024911.

——, and T. Cowan, 2006: The SAM and regional rainfall in IPCC AR4 models: Can anthropogenic forcing account for southwest Western Australian winter rainfall reduction? *Geophys. Res. Lett.,* **33,** L24708, doi:10.1029/2006GL028037.

——, and ——, 2007: Trends in Southern Hemisphere circulation in IPCC AR4 models over 1950–99: Ozone depletion versus greenhouse forcing. *J. Climate,* **20,** 681–693.

——, and ——, 2008a: Evidence of impacts from rising temperature on inflows to the Murray-Darling Basin. *Geophys. Res. Lett.,* **35,** L07701, doi:10.1029/2008GL033390.

——, and ——, 2008b: Dynamics of late autumn rainfall reduction over southeastern Australia. *Geophys. Res. Lett.,* **35,** L09708, doi:10.1029/2008GL033727.

——, H. H. Hendon, and G. Meyers, 2005a: Indian Ocean dipolelike variability in the CSIRO Mark 3 coupled climate model. *J. Climate,* **18,** 1449–1468.

——, G. Shi, T. Cowan, D. Bi, and J. Ribbe, 2005b: The response of the Southern Annular Mode, the East Australian Current, and the southern mid-latitude ocean circulation to global warming. *Geophys. Res. Lett.,* **32,** L23706, doi:10.1029/2005GL024701.

——, P. van Rensch, and T. Cowan, 2011a: Influence of global-scale variability on the subtropical ridge over southeast Australia. *J. Climate,* **24,** 6035–6053.

——, ——, ——, and H. Hendon, 2011b: Teleconnection pathways of ENSO and the IOD and the mechanisms for impacts on Australian rainfall. *J. Climate,* **24,** 3910–3923.

——, T. Cowan, and M. Thatcher, 2012: Rainfall reductions over Southern Hemisphere semi-arid regions: The role of subtropical dry zone expansion. *Sci. Rep.,* **2,** 702, doi:10.1038/srep00702.

Drosdowsky, W., 2005: The latitude of the subtropical ridge over eastern Australia: The L-index revisited. *Int. J. Climatol.,* **25,** 1291–1299.

Fauchereau, N., S. Trzaska, Y. Richard, P. Roucou, and P. Camberlin, 2003: Sea-surface temperature co-variability in the southern Atlantic and Indian Oceans and its connections with the atmospheric circulation in the Southern Hemisphere. *Int. J. Climatol.,* **23,** 663–677.

Frederiksen, J. S., C. S. Frederiksen, S. L. Osbrough, and J. M. Sisson, 2011: Changes in Southern Hemisphere Rainfall, Circulation and Weather Systems. *Proc. 19th Int. Congress on Modelling and Simulation,* Perth, Australia, Modelling and Simulation Society of Australia and New Zealand, 2712–2718.

Fu, Q., C. M. Johanson, J. M. Wallace, and T. Reichler, 2006: Enhanced mid-latitude tropospheric warming in satellite measurements. *Science,* **312,** 1179.

Ghil, M., and K. C. Mo, 1991: Intraseasonal oscillations in the global atmosphere. Part II: Southern Hemisphere. *J. Atmos. Sci.,* **48,** 780–790.

Gillett, N. P., and D. W. J. Thompson, 2003: Simulation of recent Southern Hemisphere climate change. *Science,* **302,** 273–275.

Hendon, H. H., D. W. J. Thompson, and M. C. Wheeler, 2007: Australian rainfall and surface temperature variations associated with the Southern Hemisphere annular mode. *J. Climate,* **20,** 2452–2467.

Hermes, J. C., and C. J. C. Reason, 2005: Ocean model diagnosis of interannual coevolving SST variability in the south Indian and South Atlantic Oceans. *J. Climate,* **18,** 2864–2882.

Hu, Y., and Q. Fu, 2007: Observed poleward expansion of the Hadley circulation since 1979. *Atmos. Chem. Phys., **7***, 5229–5236.

Johanson, C. M., and Q. Fu, 2009: Hadley cell widening: Model simulations versus observations. *J. Climate, **22***, 2713–2725.

Jones, D. A., W. Wang, and R. Fawcett, 2009: High-quality spatial climate data-sets for Australia. *Aust. Meteor. Oceanogr. J., **58***, 233–248.

Kajikawa, Y., B. Wang, and J. Yang, 2010: A multi-time scale Australian monsoon index. *Int. J. Climatol., **30***, 1114–1120.

Kalnay, E., and Coauthors, 1996: The NCEP/NCAR 40-Year Reanalysis Project. *Bull. Amer. Meteor. Soc., **77***, 437–471.

Kang, S. M., L. M. Polvani, J. C. Fyfe, and M. Sigmond, 2011: Impact of polar ozone depletion on subtropical precipitation. *Science, **332***, 951–954, doi:10.1126/science.1202131.

Karoly, D. J., 1989: Southern Hemisphere circulation features associated with El Niño-Southern Oscillation events. *J. Climate, **2***, 1239–1252.

Larsen, S. H., and N. Nicholls, 2009: Southern Australian rainfall and the subtropical ridge: Variations, interrelationships, and trends. *Geophys. Res. Lett., **36***, L08708, doi:10.1029/2009GL037786.

Li, Y., W. Cai, and E. P. Campbell, 2005: Statistical modeling of extreme rainfall in southwest Western Australia. *J. Climate, **18***, 852–863.

Lu, J., G. A. Vecchi, and T. Reichler, 2007: Expansion of the Hadley cell under global warming. *Geophys. Res. Lett., **34***, L06805, doi:10.1029/2006GL028443.

Marshall, G. J., 2003: Trends in the southern annular mode from observations and reanalyses. *J. Climate, **16***, 4134–4143.

Meneghini, B., I. Simmonds, and I. N. Smith, 2007: Association between Australian rainfall and the southern annular mode. *Int. J. Climatol., **27***, 109–121.

Miller, R. L., G. A. Schmidt, and D. T. Shindell, 2006: Forced annular variations in the 20th century Intergovernmental Panel on Climate Change Fourth Assessment Report models. *J. Geophys. Res., **111***, D18101, doi:10.1029/2005JD006323.

Murphy, B. F., and B. Timbal, 2008: A review of recent climate variability and climate change in southeastern Australia. *Int. J. Climatol., **28***, 859–879.

Nicholls, N., 1989: Sea surface temperature and Australian winter rainfall. *J. Climate, **2***, 965–973.

——, 2009: Local and remote causes of the southern Australian autumn-winter rainfall decline, 1958–2007. *Climate Dyn., **34***, 835–845, doi:10.1007/s00382-009-0527-6.

Rayner, N. A., D. E. Parker, E. B. Horton, C. K. Folland, L. V. Alexander, D. P. Rowell, E. C. Kent, and A. Kaplan, 2003: Global analyses of sea surface temperature, sea ice, and night marine air temperature since the late nineteenth century. *J. Geophys. Res., **108***, doi:10.1029/2002JD002670.

Reason, C. J. C., 2001: Subtropical Indian Ocean SST dipole events and southern African rainfall. *Geophys. Res. Lett., **28***, 2225–2227.

Risbey, J., M. Pook, P. McIntosh, C. Ummenhofer, and G. Meyers, 2009a: Characteristics and variability of synoptic features associated with cool season rainfall in southeastern Australia. *Int. J. Climatol., **29***, 1595–1613.

——, ——, ——, M. Wheeler, and H. Hendon, 2009b: On the remote drivers of rainfall variability in Australia. *Mon. Wea. Rev., **137***, 3233–3253.

Simmonds, I., and E. P. Lim, 2009: Biases in the calculation of Southern Hemisphere mean baroclinic eddy growth rate. *Geophys. Res. Lett., **36***, L01707, doi:10.1029/2008GL036320.

Smith, I. N., L. Wilson, and R. Suppiah, 2008: Characteristics of the northern Australian rainy season. *J. Climate, **21***, 4298–4311.

Speer, M. S., L. M. Leslie, and A. O. Fierro, 2011: Australian east coast rainfall decline related to large scale climate drivers. *Climate Dyn., **36***, 1419–1429.

Thompson, D. W. J., and S. Solomon, 2002: Interpretation of recent Southern Hemisphere climate change. *Science, **296***, 895–899.

Timbal, B., and H. Hendon, 2011: The role of tropical modes of variability in recent rainfall deficits across the Murray-Darling Basin. *Water Resour. Res., **47***, W00G09, doi:10.1029/2010WR009834.

——, B. Murphy, K. Braganza, H. Hendon, M. Wheeler, and C. Rakich, 2007: Final report for project 1.1.2. South-Eastern Australian Climate Initiative Tech. Rep., 19 pp.

Venegas, S., L. A. Mysak, and D. N. Straub, 1997: Atmosphere–ocean coupled variability in the South Atlantic. *J. Climate, **10***, 2904–2920.

Wang, B., I. S. Kang, and J. Y. Lee, 2004: Ensemble simulations of Asian–Australian monsoon variability by 11 AGCMs. *J. Climate, **17***, 803–818.

Yu, J., G. Fu, W. Cai, and T. Cowan, 2010: Impacts of precipitation and temperature changes on annual streamflow in the Murray–Darling basin. *Water Int., **35***, 313–323.

Zhang, H., 2009: Diagnosing Australia-Asian monsoon onset/retreat using large-scale wind and moisture indices. *Climate Dyn., **35***, 601–618, doi:10.1007/s00382-009-0620-x.